

Cygnus X-2, super-Eddington mass transfer, and pulsar binaries

A. R. King¹ & H. Ritter²

¹ *Astronomy Group, University of Leicester, Leicester, LE1 7RH*

² *Max-Planck-Institut für Astrophysik, Karl-Schwarzschild-Str. 1, D-85740 Garching, Germany*

3 December 2018

ABSTRACT

We consider the unusual evolutionary state of the secondary star in Cygnus X-2. Spectroscopic data give a low mass ($M_2 \simeq 0.5 - 0.7M_\odot$) and yet a large radius ($R_2 \simeq 7R_\odot$) and high luminosity ($L_2 \simeq 150L_\odot$). We show that this star closely resembles a remnant of early massive Case B evolution, during which the neutron star ejected most of the $\sim 3M_\odot$ transferred from the donor (initial mass $M_{2i} \sim 3.6M_\odot$) on its thermal time-scale $\sim 10^6$ yr. As the system is far too wide to result from common-envelope evolution, this strongly supports the idea that a neutron star efficiently ejects the excess inflow during super-Eddington mass transfer. Cygnus X-2 is unusual in having had an initial mass ratio $q_i = M_{2i}/M_1$ in a narrow critical range near $q_i \simeq 2.6$. Smaller q_i lead to long-period systems with the former donor near the Hayashi line, and larger q_i to pulsar binaries with shorter periods and relatively massive white dwarf companions. The latter naturally explain the surprisingly large companion masses in several millisecond pulsar binaries. Systems like Cygnus X-2 may thus be an important channel for forming pulsar binaries.

Key words: binaries: close – stars: evolution – stars: individual (Cygnus X-2) – stars: pulsars: general – X-rays: stars

1 INTRODUCTION

Cygnus X-2 is a persistent X-ray binary with a long orbital period ($P = 9.84$ d, Cowley, Crampton & Hutchings 1979). The observation of unambiguous Type I X-ray bursts (Smale, 1998) shows that the accreting component is a neutron star rather than a black hole. The precise spectroscopic information found by Casares, Charles & Kuulkers (1998), and the parameters which can be derived from it, is summarized in Table 1. The mass ratio $q = M_2/M_1 \simeq 0.34$ implies that mass transfer widens the system, and is therefore probably driven by expansion of the secondary star. Normally in long-period low-mass X-ray binaries (LMXBs) this occurs because of the nuclear evolution of a subgiant secondary along the Hayashi line, with typical effective temperatures $T_{\text{eff},2} \simeq 3000 - 4000$ K. However Casares et al.’s observations show that this cannot be the case for Cygnus X-2. The secondary is in the Hertzsprung gap (spectral type A9 III): use of Roche geometry and the Stefan–Boltzmann law gives $L_2 \simeq 150L_\odot$ with $T_{\text{eff},2} \simeq 7330$ K (see Table 1). Moreover the mass ratio $q \simeq 0.34$, and the assumption that the primary is a neutron star and thus obeys $M_1 \lesssim 2M_\odot$, implies that the secondary has a low mass ($M_2 = qM_1 \lesssim 0.68M_\odot$). In contrast, an isolated A9 III star would have a mass of about $4M_\odot$. More recently Orosz

& Kuulkers (1998) have modelled the ellipsoidal variations of the secondary and thereby derived a model-dependent inclination of $i = 62.5^\circ \pm 4^\circ$ which translates into component masses ($M_1 = 1.78 \pm 0.23M_\odot$ and $M_2 = 0.60 \pm 0.13M_\odot$).

In this paper we consider explanations for the unusual nature of the secondary in Cygnus X-2. We find only one viable possibility, namely that this star is currently close to the end of early massive Case B mass transfer, and thus that the neutron star has somehow managed to reject most of the mass ($\sim 3M_\odot$) transferred to it in the past. In support of this idea, we show that this type of evolution naturally explains the surprisingly large companion masses in several millisecond pulsar binaries.

2 MODELS FOR CYGNUS X-2

In this Section we consider four possible explanations for the unusual nature of the secondary in Cygnus X-2. We shall find that three of them are untenable, and thus concentrate on the fourth possibility.

Table 1. Observed and derived properties of Cygnus X-2.

spectroscopic period P	$9^d.844(\pm 3)$
radial-velocity amplitude K_2	$88.0 \pm 1.4 \text{ km s}^{-1}$
rotational velocity $v_2 \sin i$	$34.2 \pm 2.5 \text{ km s}^{-1}$
spectral type Sp(2)	A9 \pm 2 III
mass ratio $q = M_2/M_1$	0.34 ± 0.04
effective temperature $T_{\text{eff},2}$	$(7330 \pm 320) \text{ K}$
primary mass M_1	$\gtrsim (1.43 \pm 0.10)M_\odot$
secondary mass M_2	$\gtrsim (0.49 \pm 0.07)M_\odot$ $\lesssim (0.68 \pm 0.08)M_\odot$
secondary radius R_2	$8.93R_\odot \left(\frac{M_2}{M_\odot}\right)^{1/3}$
secondary luminosity L_2	$207.7L_\odot \left(\frac{M_2}{M_\odot}\right)^{2/3} \left(\frac{T_{\text{eff},2}}{7330 \text{ K}}\right)^4$

2.1 A normal star at the onset of Case B mass transfer?

The simplest explanation is that the position of the secondary in the HR diagram is just that of a normal star crossing the Hertzsprung gap. Since such a star no longer burns hydrogen in the core, this is a massive Case B mass transfer as defined by Kippenhahn & Weigert (1967), hereafter KW. Provided that the initial mass ratio $q_i \lesssim 1$ the binary always expands on mass transfer, which occurs on a thermal time-scale. Kolb (1998) investigated this type of evolution systematically and found that the secondary’s position on the HR diagram is always close to that of a single star of the same instantaneous mass. For Cygnus X-2 the A9 III spectral type would require a current secondary mass $M_2 \simeq 4M_\odot$, and thus a primary mass $M_1 = M_2/q \simeq 12M_\odot$. This is far above the maximum mass for a neutron star and would require the primary to be a black hole, in complete contradiction to the observation of Type I X-ray bursts from Cygnus X-2 (Smale, 1998).

We conclude that the secondary of Cygnus X-2 cannot be a normal star. Accordingly we must consider explanations in which it is far bigger and more luminous than expected from its estimated mass $\sim (0.49 - 0.68)M_\odot$.

2.2 A stripped subgiant?

The type of Case B evolution described in subsection (2.1) above is known as ‘early’, in that mass transfer starts when the donor’s envelope is still largely radiative rather than convective (as it would become as the star approached the Hayashi line), and ‘massive’, meaning that the helium core has a large enough mass that upon core contraction it does not become degenerate but instead ignites central helium burning. The corresponding minimum core mass is about $0.35M_\odot$, corresponding to a total ZAMS mass of $2 - 2.5M_\odot$ (depending on the assumed degree of convective overshooting during central hydrogen burning). For lower initial masses we have ‘low-mass’ Case B (Kippenhahn, Kohl & Weigert 1967). Here the donor’s helium core becomes degenerate and the envelope is convective. After a possible early rapid mass transfer phase in which the binary mass ratio $q = M_2/M_1$ is reduced to $\lesssim 1$, (Bhattacharya & van den Heuvel, 1991; Kalogera & Webbink, 1996) the donor reaches the Hayashi line and mass transfer is driven by its nuclear expansion under hydrogen shell burning. The star remains on the Hayashi line, increasing its radius and the binary pe-

riod as its core mass grows. Webbink, Rappaport & Savonije (1983) describe this type of ‘stripped giant/subgiant’ evolution in detail, and indeed fit Cygnus X-2 in this way. However there is a clear discrepancy between the observed effective temperature and that required for a Hayashi-line donor, which should be about 4100 K in this case. Webbink et al. (1983) appeal to X-ray heating by the primary to raise the temperature to the observed 7330 K, but remark that since the heating only operates on the side of the secondary facing the primary, one would expect a much larger orbital modulation of the optical flux than actually observed ($\Delta V_{\text{obs}} \simeq 0.3 \text{ mag}$) unless the orbital inclination i is low. Simple estimates (see the Appendix) show that such a small modulation would require $i < 13.4^\circ$. However the mass function and mass ratio for Cygnus X-2 can be combined to show that $M_1 \sin^3 i = (1.25 \pm 0.09)M_\odot$, so such small inclinations would imply $M_1 > 100M_\odot$, again clearly incompatible with the very strong observational evidence for a neutron star primary. A still stronger argument can be constructed on the basis that the spectral type of the secondary is not observed to vary during the orbital cycle.

2.3 A helium white dwarf undergoing a hydrogen shell flash?

It is known that newly-born helium white dwarfs can undergo one or more hydrogen shell flashes during their evolution from the giant branch to the white dwarf cooling sequence. During these flashes the star has a much larger photosphere. Calculations by Driebe et al. (1998) show that only low-mass He white dwarfs in the interval $0.21M_\odot \lesssim M_{\text{WD}} \lesssim 0.30M_\odot$ can undergo such a flash which in turn can put the star in the same position on the HR diagram as the secondary of Cygnus X-2 (e.g. the first shell flash of the sequence with $M_{\text{WD}} = 0.259M_\odot$). However, the required low secondary mass has a price: the observed mass ratio implies $M_1 = qM_2 \simeq (0.76 \pm 0.09)M_\odot$, much smaller than required by the mass function ($M_1 \sin^3 i = (1.25 \pm 0.09)M_\odot$). To make matters worse, the evolutionary track crosses the relevant region of the HR diagram in an extremely short time: the star’s radius expands on a time-scale $\tau = dt/d \ln R_2 \simeq 33 \text{ yr}$. Not only does this give the present system an implausibly short lifetime, the radius expansion would drive mass transfer at a rate $\sim \Delta M_{\text{H}}/\tau \sim \text{few} \times 10^{-4}M_\odot \text{ yr}^{-1}$, again totally inconsistent with observations. We conclude that the secondary of Cygnus X-2 cannot be a low-mass He white dwarf undergoing a hydrogen shell flash.

2.4 A star near the end of early massive Case B mass transfer?

We saw in subsection (2.1) above that a secondary near the *onset* of early massive Case B mass transfer (i.e. with $q \lesssim 1$ throughout) is ruled out for Cygnus X-2, as the required stellar masses conflict with observation. However, a more promising assignment is a secondary near the *end* of an early massive Case B evolution which began with $q_i \gtrsim 1$.

KW have investigated this process in detail. In contrast to the case $q_i \lesssim 1$ discussed by Kolb (1998), and considered in (2.1) above, the ratio $q_i \gtrsim 1$ means that the binary and Roche lobe initially shrink on mass transfer. Adiabatic stability is nevertheless ensured because the secondary’s deep

radiative envelope (‘early’ Case B) contracts on rapid mass loss. Mass transfer is therefore driven by the thermal-time-scale expansion of the envelope, but is more rapid than for $q_i \lesssim 1$ because of the orbital shrinkage. Once M_2 is reduced to the point that $q \lesssim 1$, the Roche lobe begins to expand. This slows the mass transfer, and shuts it off entirely when the lobe reaches the thermal-equilibrium radius of the secondary, since the latter then has no tendency to expand further (except possibly on a much longer nuclear time-scale). Calculations by KW and Giannone, Kohl & Weigert (1968), hereafter GKW, show that in some cases the orbit can shrink so much that the process ends in the complete exhaustion of the donor’s hydrogen envelope, ultimately leaving the core of the secondary in a detached binary. Alternatively, the rapid Case B mass transfer may end with the donor on the Hayashi line, still retaining a large fraction of its original hydrogen envelope. However, there will be no long-lasting phase of mass transfer with the donor on the Hayashi line because the star starts shrinking with ignition of central helium burning (KW). Neither of these two cases describes Cygnus X-2. However, there is an intermediate possibility: the initial mass ratio q_i may be such that the donor retains a small but non-negligible hydrogen envelope as mass transfer slows. The current effective temperature of 7330 K shows that the companion’s envelope is mainly radiative, with only a very thin surface convection zone. (A paper in preparation by Kolb et al. shows this in detail.) In the example computed by KW the donor, at the end of mass transfer, is not on the Hayashi line, but at almost the same point in the HR diagram as it occupied immediately before mass transfer began (this is confirmed by the detailed numerical calculations of Kolb et al.). Just before the process ends we then have an expanding low-mass donor, driving a modest mass transfer rate in a long-period expanding binary, but at the HR diagram position of a much more massive normal star. As we shall show below, for an initial donor mass of about $3.6M_\odot$ the end point of such an evolution can be made to match closely that observed for the secondary of Cygnus X-2. (Note that we have not performed detailed numerical calculations for this paper, but rather used the results of KW and GKW. The forthcoming paper by Kolb et al. reports detailed calculations.)

Clearly this idea offers a promising explanation of the secondary in Cygnus X-2. However there is an obvious difficulty in accepting it immediately. KW’s calculations assumed that the total binary mass and angular momentum were conserved, and in particular that the primary retained all the mass transferred to it. But the primary of Cygnus X-2 is known to be a neutron star, with a mass presumably $\lesssim 2M_\odot$, so we must require instead that it accretes relatively little during mass transfer. This agrees with the idea that a neutron star cannot accrete at rates greatly in excess of its Eddington limit ($\sim 10^{-8}M_\odot \text{ yr}^{-1}$), and the fact that almost all of the mass is transferred at much higher rates ($\gtrsim 10^{-6}M_\odot \text{ yr}^{-1}$). We thus follow earlier authors (Bhattacharya & van den Heuvel, 1991; Kalogera & Webbink, 1996) in postulating that the neutron star is extremely efficient in ejecting most of the super-Eddington mass transfer, rather than allowing the excess mass to build up into a common envelope. Clearly common-envelope evolution could not produce Cygnus X-2: the current binary period of 9.8 d shows that far too little orbital energy could have been re-

leased to remove the envelope of any plausible progenitor for the secondary (see e.g. Section 4 below). By contrast, it is at least energetically possible to expel most of a super-Eddington mass transfer rate, provided that this is done at large enough distance R_{ej} from the neutron star. If the matter is given just the escape velocity at R_{ej} the ratio of ejection to accretion rate is

$$\frac{\dot{M}_{\text{ej}}}{\dot{M}_{\text{acc}}} = \frac{R_{\text{ej}}}{R_*}, \quad (1)$$

where R_* is the radius of the neutron star. Ejecting all but about 1% of the transferred matter thus requires

$$R_{\text{ej}} \gtrsim 100R_* \sim 10^8 \text{ cm} \quad (2)$$

which is far smaller than the size of the accretion disc around the neutron star for example. (This point is discussed further by King and Begelman, 1999.)

In the next section we will consider an early massive Case B evolution for Cygnus X-2. We will find that the hypothesis of efficient mass ejection by the neutron star allows excellent agreement with the current state of the system, as well as plausible explanations for the observed states of several detached pulsar binaries.

3 EARLY MASSIVE CASE B EVOLUTION FOR NEUTRON-STAR BINARIES

The main features of early massive Case B evolution can be understood by considering the relative expansion or contraction of the donor’s Roche lobe R_L and the thermal equilibrium radius $R_{2,e}$ which the donor attains at the end of mass transfer (see e.g. GKW). As discussed above, we assume that the neutron star ejects any super-Eddington mass inflow. Since the mass transfer rate exceeds the Eddington limit by factors $\gtrsim 100$ (see above), almost all of the transferred mass must be ejected, and to an excellent approximation we can assume that the neutron star mass M_1 remains fixed during the mass transfer (the equation for R_L can actually be integrated exactly even without this assumption, but at the cost of some algebraic complexity). We assume further that the ejected mass carries the specific angular momentum of the neutron star’s orbit. This is very reasonable, since the ejection region is much smaller than the size of the disc (see eq. 2). Then we can use the result quoted by Kalogera & Webbink (1996) to write

$$\frac{R_L}{R_{L,i}} = \left(\frac{M_{2i}}{M_2}\right)^{5/3} \left(\frac{M_1}{M}\right)^{4/3} e^{2(M_2 - M_{2i})/M_1}, \quad (3)$$

where M_2 and $M = M_1 + M_2$ are the donor and total binary mass at any instant, and M_{2i}, M_1 their values at the onset of mass transfer. In writing (3) we have used the simple approximation $R_L/a \propto (M_2/M)^{1/3}$, where a is the binary separation. Using this and Kepler’s law we get the change of binary period P as

$$\frac{P}{P_i} = \left(\frac{R_L}{R_{L,i}}\right)^{3/2} \left(\frac{M_{2i}}{M_2}\right)^{1/2} \quad (4)$$

so that

$$\frac{P}{P_i} = \left(\frac{M_{2i}}{M_2}\right)^3 \left(\frac{M_1}{M}\right)^2 e^{3(M_2 - M_{2i})/M_1}. \quad (5)$$

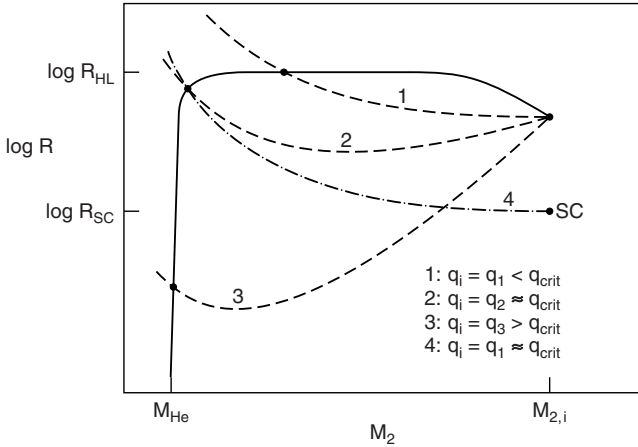


Figure 1. Schematic mass radius diagram of early massive Case B evolution showing different outcomes of mass transfer depending on the initial mass ratio q_i and initial separation. Full line: thermal equilibrium radius $R_{2,e}$ of a star with hydrogen shell burning and a non-degenerate He core of mass M_{He} as a function of total mass M_2 (generalized main sequence). R_{HL} is the maximum radius attained at the Hayashi line, R_{SC} the radius at the Schönberg–Chandrasekhar limit. Dashed lines: Roche lobe radius R_L as a function of M_2 for three different values of the initial mass ratio q_i and the maximum possible orbital separation. The dashed lines can be shifted downwards by an arbitrary amount subject to the condition that $R_{2i} \geq R_{\text{SC}}$. Dash-dotted line: mass transfer starting when the secondary has just reached the Schönberg–Chandrasekhar limit. This example shows that q_{crit} as defined in section 3 depends on the initial orbital separation of the binary.

Conventional massive Case B evolution always begins with a mass ratio $q_i = M_{2i}/M_1$ sufficiently large that R_L initially shrinks. From (3) it is easy to show that this requires $q_i > 1.2$. If during the evolution M_2 decreases enough that $q < 1.2$, R_L begins to expand again. The curves of $\log R_L$ thus have the generic U-shaped forms shown in Figs. 1 – 3.

The thermal equilibrium radius $R_{2,e}$ depends on the relative mass M_{He}/M_2 of the donor’s helium core. Figs. 1 – 3 show the so-called ‘generalized main sequences’ of GKW, the first schematically, and the latter two for $M_{2i} = 3M_{\odot}, 5M_{\odot}$. For a core-envelope structure to be applicable, the star must have at least finished central hydrogen burning. Since the mass transfer takes place on the thermal time-scale of the donor there is little nuclear evolution, and we can regard M_{He} as fixed. The quantity $R_{2,e}$ shown in Figs. 1 – 3 therefore gives the thermal equilibrium radius attained by the star after transferring varying amounts of its hydrogen envelope. The evolution of the system is now specified by the initial mass ratio q_i and the radius R_{2i} of the donor at the onset of mass transfer. This can lie between the maximum radius R_B reached during central hydrogen burning and one almost as large as the value R_{HL} at the Hayashi line (mass transfer is adiabatically unstable if the donor develops a deep convective envelope). The allowed initial radius range is about a factor 2 for a donor with $M_{2i} = 2.5M_{\odot}$, increasing to a factor ~ 6 for $M_{2i} = 5M_{\odot}$ (Bressan et al. 1993).

We see from the schematic Fig. 1 that three qualitatively different outcomes of early massive Case B mass transfer are possible:

1. ‘small’ q_i , i.e. M_{2i} only slightly larger than M_1 . Here the Roche lobe soon begins to expand, so the curves of $\log R_L$ and $\log R_{2,e}$ cross before much mass is transferred. Mass transfer ends with ignition of central helium burning as this makes the star shrink somewhat. At this point the secondary still has a thick hydrogen envelope and lies on the Hayashi line, with the binary having a long orbital period. During central helium burning the secondary stays on the Hayashi line but remains detached. Mass transfer resumes only after central helium burning when the star approaches the asymptotic giant branch (AGB). Mass transfer is again driven by nuclear evolution (double shell-burning). Since core helium-burning has ceased this is Case C. Here (unusually) the mass transfer is adiabatically stable, despite the secondary’s deep convective envelope, since the mass ratio is already $\lesssim 1$. The average mass transfer rate is again of order $10^{-6}M_{\odot} \text{ yr}^{-1}$, but may become up to an order of magnitude higher during thermal pulses (Pastetter & Ritter 1989). The donor may also lose large amounts of envelope mass in a wind. If the binary again manages to avoid common-envelope evolution by ejecting most of the transferred mass, mass transfer will finally end once the secondary’s envelope has been lost, leaving a very wide (period $\sim 10 \text{ yr}$) binary containing a neutron star and a CO white dwarf.

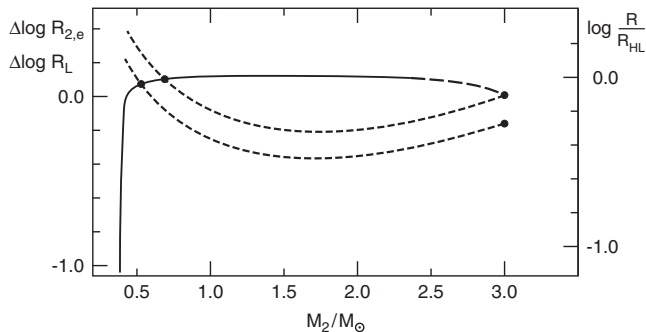
2. ‘critical’ q_i . We define this as the case where the $R_L, R_{2,e}$ curves cross at the ‘knee’ in the mass–radius curve, i.e. with M_2 only slightly larger than M_{He} , so the mass transfer depletes almost the entire envelope. The remnant donor retains a thin hydrogen envelope, and lies between the main sequence and the Hayashi line on the HR diagram. Thus the envelope mass is low enough to prevent the star lying on the Hayashi line, but not so low that the remnant is small and hot, i.e. to the left of the main sequence. The initial separation must be small enough that mass transfer starts before central helium burning, but large enough that it starts only after the donor has reached the Schönberg–Chandrasekhar limit. This limit is defined as the point where the isothermal helium core has reached the maximum mass which is able to support the overlying layers of the star, i.e. the point at which core collapse begins. The orbital period is shorter than in case 1., but longer than in case 3. below. Cygnus X-2 is an example of this evolution, viewed at the point where the donor has almost attained its thermal-equilibrium radius, and mass transfer is well below the maximum thermal-time-scale rate. This evolution ends with nuclear evolution of the donor to smaller radii as the mass of the hydrogen-rich envelope is further reduced by shell burning. The system detaches, leaving a helium-star remnant which subsequently ignites central helium burning and finally becomes a CO white dwarf.

3. ‘large’ q_i . The curves cross only when the hydrogen envelope is effectively exhausted. The remnant is a helium star and the orbital period is short. If $M_{\text{He}} \lesssim 0.9M_{\odot}$ the helium star evolves directly into a CO white dwarf. If $M_{\text{He}} \gtrsim 1M_{\odot}$ this star re-expands during helium shell-burning. This in turn can give rise to a further phase of (so-called Case BB) mass transfer, e.g. Delgado & Thomas, 1981; Law & Ritter, 1983; Habets, 1985, 1986).

Table 2 summarizes the possible Case B evolutions with a neutron-star primary. The various outcomes all reflect the general tendency of larger q_i (i.e. larger M_{2i}) to produce greater orbital contraction, and thus smaller and relatively

Table 2. Outcomes of Case B evolution with a neutron-star primary

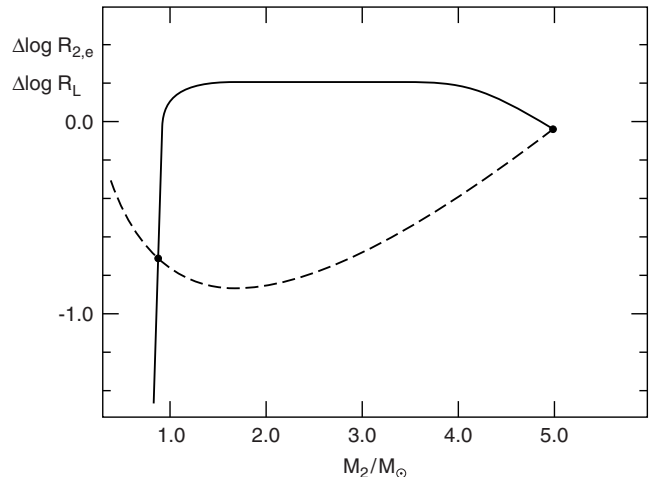
subcase	intermediate stages	P_f (d)	final WD companion
low mass	Hayashi-line LMXB	$\sim 10 - 1000$	He, obeys mass-period relation
early massive, $q_i < q_{\text{crit}}$	Hertzsprung-gap XRB, Case C mass transfer	$\gtrsim 1000$	CO, obeys mass-period relation
early massive, $q_i \simeq q_{\text{crit}}$	Cygnus X-2	~ 10	CO, overmassive
early massive, $q_i > q_{\text{crit}}$	NS + He star, Case BB mass transfer?	$\lesssim 1 - 10$,	CO, overmassive


Figure 2. Mass-radius diagram for early massive Case B evolution. Full (and long dashed) line: generalized main sequence for $3M_{\odot}$ stars taken from GKW. Short dashed lines: Roche lobe radius R_L as a function of M_2 computed from (3) with $M_1 = 1.4M_{\odot}$, $M_{2i} = 3M_{\odot}$ for two values of R_{2i} ($0.75R_{\text{HL}}$ and $0.55R_{\text{HL}}$).

less massive remnants (their mass is a smaller fraction of a larger M_{2i}) and short orbital periods. Conversely, larger R_{2i} in the range $R_B - R_{\text{HL}}$, where R_B is the maximum radius reached during central hydrogen burning, produces exactly the opposite trends. To model Cygnus X-2 one thus needs q_i close to the critical value.

As can be seen from the following arguments the range of possible solutions is strongly constrained by equation (3): with the assumption that M_1 remains essentially constant during the evolution, M_{2f} is fixed by the observed mass ratio $q_f = 0.34 \pm 0.04$. On the other hand, q_i is also essentially fixed by the model assumption that the current donor is close to the end of Case B mass transfer. This in turn means that the donor is now close to thermal equilibrium, with its luminosity therefore coming mainly from hydrogen shell burning.

Use of the generalized main sequence for $3M_{\odot}$ stars given in GKW (their fig. 7, shown here in Fig. 2) demonstrates that one can account for the current state of the donor in Cygnus X-2 if this star had $M_{2i} \simeq 3M_{\odot}$ (i.e. $q_i \simeq 2.1$) and $0.55R_{\text{HL}} \lesssim R_{2i} \lesssim 0.75R_{\text{HL}}$ when mass transfer began, corresponding roughly to $0.5M_{\odot} \lesssim M_{2f} \lesssim 0.7M_{\odot}$. The numerical results of GKW (their Table 2 and Fig. 4) suggest that the current state of the donor is then given approximately by $M_2 = 0.79M_{\odot}$, $M_{\text{He}} = 0.67M_{\odot}$ and thus $q_0 = M_{\text{He}}/M_2 = 0.85$; with $T_{\text{eff},2} = 7060$ K, $L_2 = 126L_{\odot}$ and $R_2 = 7.5R_{\odot}$. These values correspond to an orbital period $P \simeq 8.4$ d. From (5) we infer that mass transfer started at an orbital period $P_1 \simeq 3.5$ d. These quantities are


Figure 3. Mass-radius diagram for early massive Case B evolution. Full line: generalized main sequence for $5M_{\odot}$ stars taken from GKW. Short dashed line: Roche lobe radius R_L as a function of M_2 computed from (3) with $M_1 = 1.4M_{\odot}$, $M_{2i} = 5M_{\odot}$.

close to those given in Table 1, although the predicted M_2 is slightly larger than the observational estimate. This may either result from the fact that the chemical composition of the models defining the generalized main sequences is characterized by a step function at $M_r = M_c$ and thus differs from that of evolutionary models, or from the fact that the initial chemical composition ($X = 0.602$, $Z = 0.044$) and the opacities used by GKW are rather outdated. In addition the core mass $M_{\text{He}} = 0.67M_{\odot}$ inferred above points to an initial mass higher than the $\sim 3M_{\odot}$ suggested earlier. In fact to fit the observed value of $0.5M_{\odot} \lesssim M_{2f} \lesssim 0.7M_{\odot}$, more modern calculations than those of GKW (e.g. Bressan et al. 1993) yield the required core mass if the initial mass was $3.2 \lesssim M_{2i} \lesssim 4.1M_{\odot}$.

We conclude that the observational data for Cygnus X-2 are well reproduced if we assume it is a remnant of early massive Case B evolution with q_i close to the critical value $\sim 2.3 - 2.9$, if $M_1 \sim 1.4M_{\odot}$, or $\sim 1.8 - 2.3$, if we adopt the value $M_1 \sim 1.8M_{\odot}$ derived by Orosz & Kuulkers (1998). For the remainder of this paper we shall adopt $M_1 = 1.4M_{\odot}$.

4 END PRODUCTS

The discussion above shows that for both low-mass Case B, and for early massive Case B with q_i below a critical value

Table 3. Binary pulsars with relatively massive WD companions

pulsar	P (d)	M_2 (M_\odot)	P_s (ms)
J0621+1002	8.32	> 0.45	28.8
J1022+1001	7.81	> 0.73	16.5
J2145-0750	6.84	> 0.43	16.1
B0655+64	1.03	0.7 :	196

(~ 2.6 for $M_{2i} \sim 3.6M_\odot$), the evolution leads to a long-period binary with the donor on the Hayashi line. As is well known, the luminosity and radius of such a star are fixed by its degenerate core mass M_c rather than its total mass M_2 . Even though the degenerate core is different in nature in the two cases, it is possible to give a single formula for the radius, i.e

$$r_2 = \frac{3.7 \times 10^3 m_c^4}{1 + m_c^3 + 1.75m_c^4}, \quad (6)$$

where $r_2 = R_2/R_\odot$, $m_c = M_c/M_\odot$ (Joss, Rappaport & Lewis, 1987). Then using the well-known relation

$$P = 0.38 \frac{r_2^{3/2}}{m_2^{1/2}} \text{ d} \quad (7)$$

($m_2 = M_2/M_\odot$) which follows from Roche geometry, we get a relation between M_c , M_2 and the orbital period P (e.g. King, 1988). Once all of the envelope mass has been transferred we are left with a wide binary containing a millisecond pulsar (the spun-up neutron star) in a circular orbit with the white-dwarf core of the donor. Since at the end of mass transfer we obviously have $m_2 = m_c$, such systems should obey the relation

$$P \simeq 8.5 \times 10^4 \left(\frac{m_2^{11/2}}{[1 + m_c^3 + 1.75m_c^4]^{3/2}} \right) \text{ d}. \quad (8)$$

The timing orbit of the millisecond pulsar allows constraints on the companion mass, so this relation can be tested by observation. Lorimer et al. (1995), Rappaport et al. (1995) and Burderi, King & Wynn (1996) show that while the relation is consistent with the data for a majority of the ~ 25 relevant systems, there are several systems (currently 3 or 4; see Fig. 4 and Table 3) for which the white dwarf mass is probably too large to fit. While one might possibly exclude B0655+64 because of its long spin period P_s (but see below), the other three systems are clearly genuine millisecond pulsars.

Our considerations here offer a simple explanation for this discrepancy. If the initial mass ratio q_i lies above the critical value (~ 2.6 for $M_{2i} \sim 3.6M_\odot$), the donor radius will be less than R_{HL} at the end of early massive Case B mass transfer, and the orbital period relatively shorter. When such systems finally detach from the Roche lobe, the WD companion is considerably more massive than expected for the orbital period on the basis of the Hayashi-line relation (8). We see from (5) that systems with large initial companion masses M_{2i} ($\gtrsim 4M_\odot$) can end as short-period systems. Table 4 and Fig. 4 show the expected minimum final periods P_f and companion masses M_2 for various M_{2i} , i.e. assuming that mass transfer began with the donor at the Schönberg–Chandrasekhar limit.

Table 4 and Fig. 4 show that early massive Case B evolution with q_i larger than the critical value can explain the

Table 4. Short-period end-products of early massive Case B evolution

M_{2i} (M_\odot)	P_f (min) (d)	M_2 (M_\odot)
4.0	6.60	0.56
5.0	1.25	0.79
6.0	0.268	1.05
7.0	0.048	1.46

The minimum final period P_f (min) is calculated assuming that mass transfer began at the Schönberg–Chandrasekhar limit. Initial donor masses $M_{2i} \gtrsim 4M_\odot$ may possibly be ruled out because of delayed dynamical instability (see text).

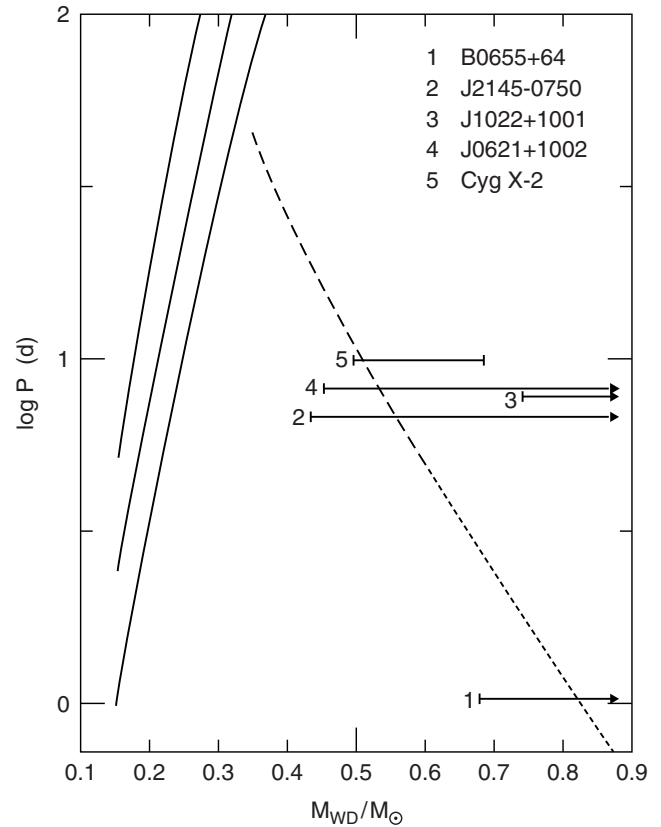


Figure 4. $P - M_2$ diagram for long-orbital-period binary ms-pulsars and Cygnus X-2. Full lines: predicted $P - M_2$ relation for systems in which the donor star evolved along the Hayashi line (taken from Rappaport et al. 1995). Dashed line: predicted *minimum* orbital period for systems in which the white dwarf secondary was formed via early massive Case B mass transfer. The short-dashed part of this curve is realised only if the neutron star can expel the transferred mass despite the binary being subject to the delayed dynamical mass transfer instability. Also shown are the (P, M_2) values of the four ‘discrepant’ ms-pulsar binaries listed in Table 3, and the current position of Cygnus X-2.

discrepant pulsar systems of Table 3. Indeed it appears that the process can end with very short orbital periods, offering an alternative to the usual assumption of a common-envelope phase (Bhattacharya, 1996; Tauris, 1996) The limiting factor for this kind of evolution may be the so-called ‘delayed dynamical instability’ (Webbink, 1977; Hjellming, 1989). For a sufficiently massive initial donor, mass transfer

eventually becomes dynamically unstable because the adiabatic mass radius exponent of a strongly stripped radiative star becomes negative and the donor begins to expand adiabatically in response to mass loss. For typical neutron star masses $M_1 \simeq 1.4M_\odot$ this would limit M_{2i} to values $\lesssim (4-4.5)M_\odot$ (Hjellming 1989; Kalogera & Webbink, 1996). Given the uncertainties in our estimates, this is probably consistent with the initial mass $M_{2i} \gtrsim 5M_\odot$ needed to explain the current state of the most extreme discrepant system (B0655+64). The other three systems can all be fitted with $M_{2i} \lesssim 4M_\odot$, so there is no necessary conflict with the mass limits for the delayed dynamical instability.

We may now ask about the end states of such an evolution if the neutron star were unable to eject the mass transferred at the very high rates expected once the delayed dynamical instability set in and the system went through a common envelope phase instead. Using the standard prescription for estimating the parameters of a post common envelope system (e.g. Webbink 1984) with the values for M_{2i} and $M_{2f} = M_2$ given in Table 4, $M_1 = 1.4M_\odot$ and $\alpha_{CE}\lambda = 0.5$, where $\lambda \sim 0.5$ is a structural parameter and α_{CE} the common envelope efficiency parameter defined by Webbink (1984), we find that the final orbital period is $0.04 \lesssim P_f(d) \lesssim 0.2$ if mass transfer set in when the donor was already near the Hayashi line, and smaller still if mass transfer set in earlier or if α_{CE} is smaller than unity. On the other hand, unless α_{CE} is significantly smaller than unity, common envelope evolution starting from a system with the donor on the asymptotic giant branch would end with periods much longer than those of the systems listed in Table 3 and shown in Fig. 4. Table 5 shows the outcome of common-envelope evolution in the two extreme cases where mass transfer starts at the Schönberg–Chandrasekhar limit, and on the Hayashi line. Although common-envelope efficiencies exceeding unity are discussed in the literature (i.e. energy sources other than the orbit are used to expel the envelope), the values found for $\beta_{CE} = \lambda \alpha_{CE}$ in Table 5 show that to produce Cyg X-2-like systems requires absurdly large efficiencies, even starting from the most distended donor possible. Thus common envelope evolution does not offer a promising explanation for these systems. Their very existence may thus indicate that an accreting neutron star can eject mass efficiently even at the very high mass transfer rates encountered in the delayed dynamical instability. We conclude therefore that even very rapid mass transfer on to a neutron star does not necessarily result in a common envelope (cf King & Begelman, 1999).

We note finally that all of the pulsars of Table 3 have spin periods much longer than their likely equilibrium periods (i.e. they lie far from the ‘spinup line’, cf Bhattacharya & van den Heuvel, 1991), suggesting that they have accreted very little mass ($\ll 0.1M_\odot$) during their evolution. This agrees with our proposal that these systems are the direct outcome of a super-Eddington mass transfer phase in which almost all the transferred mass is ejected.

5 SPACE VELOCITY AND POSITION OF CYGNUS X-2 IN THE GALAXY

The distance to Cygnus X-2 derived from the observations of Type I X-ray bursts (Smale 1989) is $d = (11.6 \pm 0.3)$ kpc.

From the galactic coordinates $l = 87.33^\circ$ and $b = -11.32^\circ$ and the solar galactocentric distance $R_0 = (8.7 \pm 0.6)$ kpc one derives a galactocentric distance for Cygnus X-2 of $d_{GC} = (14.2 \pm 0.4)$ kpc and a distance from the galactic plane of $z = (-2.28 \pm 0.06)$ kpc. Thus Cygnus X-2 has a very peculiar position indeed, being not only in the halo but also in the very outskirts of our galaxy. But not only is its position peculiar, its space velocity with respect to the galactic centre is also surprising. It can be shown that the observed heliocentric radial velocity of $\gamma = (-208.6 \pm 0.8)$ km s⁻¹ (Casares et al. 1998) is totally incompatible with prograde rotation on a circular, even inclined orbit around the galactic centre (Kolb et al., in preparation). The orbit is either highly eccentric and/or retrograde. In either case Cygnus X-2 must have undergone a major kick in the past, presumably when the neutron star was formed in a Type II supernova. Since prior to the supernova explosion the primary was much more massive ($M_{1i} \gtrsim 10M_\odot$) than the secondary ($M_{2i} \sim 3.6M_\odot$), the latter was still on the main sequence when the supernova exploded. Thus the age of Cygnus X-2 (and the time elapsed since the supernova) is well approximated by the nuclear time-scale of the secondary, which is $\sim 4 \cdot 10^8$ yr for a $\sim 3.6M_\odot$ star. This means that Cygnus X-2 must have gone around the galactic center a few times since its birth or supernova explosion and that, therefore, its birthplace in the galaxy cannot be inferred from its current position and velocity.

6 DISCUSSION

We have shown that the unusual nature of the secondary star in Cygnus X-2 can be understood if the system is near the end of a phase of early massive Case B evolution in which almost all of the transferred material is ejected. The system is unusual in having had an initial mass ratio $q_i = M_2/M_1$ in a narrow critical range near $q_i \simeq 2.6$; smaller ratios lead to detached systems with the secondary near the Hayashi line, and larger ratios produce binary pulsars with fairly short orbital periods and relatively massive white dwarf companions. During this evolution, much of the companion’s original mass ($\sim 3M_\odot$ for Cygnus X-2) is transferred and consequently lost on the thermal time-scale $\sim 10^6$ yr of this star. Evidently the huge mass loss rate and the short duration of this phase make it difficult to detect any systems in this state; they would probably resemble Wolf–Rayet stars of the WNe type (i.e. showing hydrogen).

Cygnus X-2 is currently near the end of the thermal time scale mass transfer phase, so that its mass transfer rate is now well below the thermal time-scale value, and probably given by the accretion rate. At $\dot{M}_{acc} \sim 2 \times 10^{-8}M_\odot$ yr⁻¹ (Smale, 1998), this is nevertheless one of the highest in any LMXB, making it easily detectable. Only a full calculation of the evolution, with in particular a detailed model for the secondary, can predict the duration of the current phase; this is not an easy task, as this star deviates strongly from thermal equilibrium during most of the evolution. But it is clear that the mass transfer rate will decline as the remaining few tenths of a solar mass in the hydrogen envelope are transferred. Cygnus X-2’s long orbital period and large accretion disc mean that even its current mass transfer rate only slightly exceeds the critical value required for a persis-

Table 5. Outcomes of common-envelope evolution for early massive Case B

Case	M_{2i} (M_{\odot})	M_{2f} (M_{\odot})	M_1 (M_{\odot})	R_{2i} (R_{\odot})	P_f (d) for $\beta_{\text{CE}} = 0.5$	β_{CE} for $P_f = 8$ d	β_{CE} for $P_f = 1$ d
$R_{2i} = R_{\text{SC}}$	4.0	0.56	1.4	8.5	0.0035	86.9	21.7
	5.0	0.79	1.4	10.9	0.0043	75.7	18.9
	6.0	1.05	1.4	14.2	0.0054	64.8	16.2
	7.0	1.46	1.4	16.7	0.0071	54.2	13.6
$R_{2i} = R_{\text{HL}}$	4.0	0.56	1.4	41.4	0.038	17.8	4.5
	5.0	0.79	1.4	71.0	0.071	11.7	2.9
	6.0	1.05	1.4	109.	0.12	8.5	2.1
	7.0	1.46	1.4	153.	0.20	5.9	1.5

The initial system in each case consists of a neutron star (mass M_1) a donor at the onset of massive Case B evolution (mass M_{2i} , core mass M_{2f}). In the upper half of the table mass transfer is assumed to start when the donor reaches the Schönberg–Chandrasekhar limit, corresponding to the minimum possible orbital separation. In the lower half of the table mass transfer is assumed to start only when the donor has reached the Hayashi line, corresponding to the maximum possible orbital separation. The parameter $\beta_{\text{CE}} = \lambda \alpha_{\text{CE}}$.

tent rather than a transient LMXB (cf. King, Kolb & Burderi 1996), so the system will eventually become transient. Once the envelope has been transferred, mass transfer will stop, and the system will become a pulsar binary with about the current orbital period $P = 10$ d, and a white dwarf companion with a mass which is slightly higher than that of the companion’s present helium core. Clearly since the present core mass is at least $0.35M_{\odot}$ this $P - m_2$ combination will not obey the Hayashi-line relation (8), so Cygnus X-2 will become another ‘discrepant’ system like those in Table 3.

The reasoning of the last paragraph shows that Cygnus X-2 will cease to be a persistent X-ray binary within the current mass transfer time-scale $t_{\text{M}} = (M_2 - M_c)/\dot{M}_{\text{acc}} \sim 10^7$ yr. Its past lifetime as a persistent source before the current epoch, and its future one as a detectable transient after it, are both likely to be of a similar order, although full evolutionary calculations are required to check this. The fact that we nevertheless observe even one system like Cygnus X-2 strongly suggests that the birthrate of such systems must be relatively high, i.e. $\sim 10^{-7}$ yr $^{-1}$ in the Galaxy. Since the binary pulsar end-products of these systems have enormously long lifetimes, this may suggest that systems like Cygnus X-2 play a very important role in providing the Galactic population of millisecond pulsars.

Cygnus X-2 thus fits naturally into a unified description of long-period LMXBs in which super-Eddington Case B mass transfer is efficiently ejected by the neutron star. While the ejection process can already be inferred for the formation history of Hayashi-line LMXBs resulting from low-mass Case B evolution (Bhattacharya & van den Heuvel, 1991; Kalogera & Webbink, 1996), Cygnus X-2 supplies the most powerful evidence that this process must occur. The work of Section 2 shows that it is very hard otherwise to reconcile the rather low current mass ($M_2 \simeq 0.5 - 0.7M_{\odot}$) of the secondary with its large radius ($R_2 \simeq 7R_{\odot}$) and high luminosity ($L_2 \simeq 150L_{\odot}$). From Section 4 we see that the orbital period $P = 9.84$ d is far too long for the system to be the product of common-envelope evolution, leaving no realistic alternative for driving the required mass ejection.

7 ACKNOWLEDGMENTS

ARK thanks the Max-Planck-Institut für Astrophysik for its hospitality during 1998 August, and the U.K. Particle Physics and Astronomy Research Council for a Senior Fellowship. HR thanks the Leicester University Astronomy Group for its hospitality during 1998 November/December, and support from its PPARC Short-Term Visitor grant.

8 APPENDIX: X-RAY HEATING IN CYGNUS X-2

In Section 2.2 we considered a stripped subgiant model for Cyg X-2, and asserted that the observed orbital modulation of the optical flux ($\Delta V_{\text{obs}} \simeq 0.3$ mag) would require an extremely low inclination if one appeals to X-ray heating of the companion to raise its observed effective temperature to 7330 K. Here we justify this claim.

We consider a simple picture in which the hemisphere of the (spherical) companion facing the neutron star has effective temperature 7330 K, while the other hemisphere has the Hayashi-line effective temperature 4100 K. We consider the effect of relaxing these assumptions below. Then viewing the heated face at the most favourable phase the observer sees hot and cool areas $2\pi R_2^2(1/2 + i/\pi)$, $2\pi R_2^2(1/2 - i/\pi)$, where i is the inclination in radians, with the two expressions reversing at the least favourable phase. Neglecting limb-darkening, the ratio of maximum to minimum flux is

$$\frac{F_{\text{max}}}{F_{\text{min}}} = \frac{(1/2 + i/\pi)B_{\text{hot}} + (1/2 - i/\pi)B_{\text{cool}}}{(1/2 + i/\pi)B_{\text{cool}} + (1/2 - i/\pi)B_{\text{hot}}}, \quad (9)$$

where B_{hot} , B_{cool} are the optical surface brightnesses of the hot and cool regions respectively. Approximating these by Planck functions at 5500 Å, we find $B_{\text{hot}}/B_{\text{cool}} \simeq 15$. Requiring $F_{\text{max}}/F_{\text{min}} \lesssim 1.3$ ($\Delta V_{\text{obs}} \simeq 0.3$ mag) in (9) shows that $i \lesssim 0.0745\pi$, or $i \lesssim 13.4^\circ$, as used in Section 2.2

In reality the heated region would be smaller than a hemisphere, and its temperature higher than 7330 K in order to produce an average observed temperature of this value. However relaxing these limits clearly requires even smaller inclinations than the estimate above, because the contrast in optical surface brightness between the hot and cool regions would be even larger than the ratio ~ 15 we found above.

REFERENCES

- Bhattacharya, D., van den Heuvel, E.P.J., 1991, *Phy.Rep.*, 203, 1
Bhattacharya, D., 1996, in van Paradijs, J., van den Heuvel
E.P.J., Kuulkers, E., eds., *Compact Stars in Binaries*, IAU
Symp. 165, Kluwer, Dordrecht, p. 243
Bressan, A., Fagotto, F., Bertelli, G., Chiosi, C., 1993, *A&AS*,
100, 647
Burderi, L., King, A.R., Wynn, G.A., 1996, *ApJ*, 457, 348
Casares, J., Charles, P.A., Kuulkers, E., 1998, *ApJ*, 493, L39
Cowley, A.P., Crampton, D., Hutchings, J.B., 1979, *ApJ*, 231, 539
Delgado, A.J., & Thomas, H.C., 1981, *A&A*, 96, 142
Driebe, T., Schönberner, D., Blöcker, T., Herwig, F., 1998, *A&A*,
339, 123
Giannone, P., Kohl, K., Weigert, A., 1968, *Z. Astrophys.*, 68, 107
(GKW)
Habets, G., 1985, PhD thesis, University of Amsterdam
Habets, G., 1986, *A&A*, 167, 61
Hjellming, M.S., 1989, PhD thesis, University of Illinois
Joss, P.C., Rappaport, S.A., Lewis, W., 1987, *ApJ*, 319, 180
Kalogera, V., Webbink, R.F., 1996, *ApJ*, 458, 301
King A.R., 1988, *QJRAS*, 29, 1
King, A.R., Begelman, 1999, *ApJ*, in press
King, A.R., Kolb, U., Burderi, L., 1996, *ApJ*, 464, L127
Kippenhahn, R., Weigert, A., 1967, *Z. Astrophys.*, 65, 251 (KW)
Kippenhahn, R., Kohl, K., Weigert, A., 1967, *Z. Astrophys.*, 66,
58
Kolb, U., 1998, *MNRAS*, 297, 419
Law, W.Y., Ritter, H., 1983, *A&A*, 123, 33
Lorimer, D.R., Nicastro, L., Lyne, A.G., Bailes, M., Manchester,
R.N., Johnston, S., Bell, J.F., D'Amico, N., Harrison, P.A.,
1995, *ApJ*, 439, 933
Orosz, J.A., Kuulkers, E., 1998, *MNRAS*, in press
Pastetter, L., Ritter, H., 1989, *A&A*, 214, 186
Rappaport, S., Podsiadlowski, P., Joss, P.C., Di Stefano, R., Han,
Z., 1995, *MNRAS*, 273, 731
Smale, A., 1998, *ApJ*, 498, L141
Tauris, T., 1996, *A&A* 315, 453
Webbink, R.F., 1977, *ApJ*, 211, 486
Webbink, R.F., 1984, *ApJ*, 277, 355
Webbink, R.F., Rappaport, S., Savonije, G.J., 1983, *ApJ*, 270,
678